The Astrophysical Journal, 628:L25–L28, 2005 July 20

EARLY OPTICAL-INFRARED EMISSION FROM GRB 041219a: NEUTRON-RICH INTERNAL SHOCKS AND A MILDLY MAGNETIZED EXTERNAL REVERSE SHOCK

Y. Z. Fan,[1,2,3] Bing Zhang,[3] and D. M. Wei[1,2]
Received 2005 April 6; accepted 2005 June 9; published 2005 July 6

ABSTRACT

Very early optical and near-infrared emission was discovered to have accompanied the long gamma-ray burst GRB 041219a. Here we show that the optical-IR flash tracking the gamma-ray light curve during the prompt emission can be understood as emission from neutron-rich internal shocks, as has been suggested by Fan & Wei. The early K_s-band afterglow light curve after the prompt phase can be well modeled as the superposition of a reverse and a forward shock component. The radio data also support the reverse-shock interpretation.

Subject headings: gamma rays: bursts — ISM: jets and outflows — radiation mechanisms: nonthermal

1. INTRODUCTION

GRB 041219a was detected by both the IBIS detector on the *International Gamma-Ray Astrophysics Laboratory* satellite (Gotz et al. 2004) and the *Swift* Burst Alert Telescope (BAT) (Barthelmy et al. 2004). This burst distinguishes itself from other bursts in several respects: (1) It was very bright. The 15–350 keV fluence measured by the *Swift* BAT was approximately 1.55×10^{-4} ergs cm^{-2} (Barthelmy et al. 2004), placing it in the top few percent among the 1637 GRB events listed in the comprehensive fourth Burst and Transient Source Experiment catalog (Paciesas et al. 1999). (2) The duration of the prompt γ-ray emission (T_{90}) was approximately 520 s, making it one of the longest bursts ever detected. (3) Prompt optical and infrared emission was found to accompany the prompt γ-ray emission (Vestrand et al. 2005; Blake et al. 2005). This is the first such case since GRB 990123 (e.g., Akerlof et al. 1999). (4) The location of this burst is near the Galactic plane and in a direction with high optical extinction (Galactic coordinates $l = 120°$, $b = +0\overset{\circ}{.}1$), so the R-band extinction is very large (~4.9 mag or even larger). For this reason, no late optical afterglow was detected. Fortunately, in the IR band the afterglow (including that in the very early phase) has been well detected (Blake et al. 2005). The redshift is unknown. In what follows, we assume $z = 1$.

The very early long-wavelength observation is very important for diagnosing the composition of the outflow (Fan et al. 2004; Zhang & Kobayashi 2005; Fan et al. 2005),[4] since the late afterglow, taking place hours after the burst trigger, is powered by the forward shock, so that essentially all the initial information about the ejecta is lost. In this Letter, we apply our previous analyses to discuss the very early long-wavelength observation of GRB 041219a.

2. THE PROMPT OPTICAL AND NEAR-INFRARED FLASH

There was some interest in discussing and searching for prompt long-wavelength radiation accompanying prompt γ-ray emission even in the pre-afterglow era (e.g., Katz 1994; Schaefer et al. 1994; Wei & Cheng 1997). In the afterglow era, more theoretical attention has been paid to the topic. In the standard internal-shock model, long-wavelength flashes are expected to accompany the prompt γ-ray emission (Mészáros & Ress 1997, 1999; Fan & Wei 2004a). If there is a large amount of neutrons contained in the GRB outflow, the decayed-neutron shells will provide more collisions at a larger distance from the central engine. If a burst is long enough, the neutron-rich internal shocks will give rise to detectable long-wavelength flashes during the prompt γ-ray emission phase (Fan & Wei 2004b).

In the standard internal-shock model, the synchrotron self-absorption frequency can be estimated as $\nu_a \sim 7 \times 10^{16} L_{\rm syn,52}^{2/7} \times \Gamma_{m,2.5}^{3/7} R_{\rm int,13}^{-4/7} B_4'^{1/7} [2/(1+z)]$ Hz (e.g., Li & Song 2004), where $L_{\rm syn}$ is the synchrotron radiation luminosity, Γ_m is the bulk Lorentz factor of the two merged shells, $R_{\rm int} \sim 2\Gamma_m^2 c\,\delta t/(1+z)$ is the typical internal-shock radius with δt the observed variable timescale of the prompt γ-ray light curve, B' is the comoving-frame magnetic field strength in the internal-shock phase, and the convention $Q_x = Q/10^x$ has been adopted in cgs units here and throughout. For typical GRB parameters, one can see that ν_a is usually well above the optical band. This tends to suppress the optical flux. Also, the F_ν spectrum is expected to have a power-law index 5/2, inconsistent with the prompt IR data on GRB 041219a (see Fig. 2 of Blake et al. 2005). Although, with the proper adjustment of parameters, the proton-dominated internal shock models may be able to match the observation, in this Letter we focus on an alternative interpretation, that is, the neutron-rich internal shock model (Fan & Wei 2004b).

There are good reasons to assume that large amounts of neutrons (comparable to the amount of protons) exist in GRB ejecta (see, e.g., Derishev et al. 1999; Beloborodov et al. 2003; Pruet et al. 2003). In the neutron-rich internal shock model, the Lorentz factors (LFs) of the proton shells are variable, and so are the LFs of the accompanying neutron shells. The slow neutrons (with $\Gamma_{n,s} = 50$) coupled with slow proton shells do not interact with other materials before decaying [the typical β-decay radius is $\sim(900\ {\rm s})c\Gamma_{n,s} = 1.3 \times 10^{15}$ cm, where c is the speed of light]. However, if the GRB lasts long enough, the slow neutron shells ejected at earlier times will be swept successively by the faster proton shells ejected at later times. This happens over a distance range of $\sim 10^{13}$ to several times 10^{15} cm, in which the slow neutron shells decay continuously. The proton shells interact with the β-decay products of the slow neutron shells and power detectable long-wavelength prompt emission, as shown in Fan & Wei (2004b).

[1] Purple Mountain Observatory, Chinese Academy of Sciences, 2 West Beijing Road, 210008 Nanjing, China.
[2] National Astronomical Observatories, Chinese Academy of Sciences, 20A Datun Road, 100012 Beijing, China.
[3] Department of Physics, University of Nevada, Las Vegas, 4505 Maryland Parkway, Las Vegas, NV 89154-4002.
[4] In principle, the ejecta of GRBs may be Poynting flux–dominated (see Lyutikov & Blandford 2003 and references therein), neutron-rich (e.g., Derishev et al. 1999; Beloborodov 2003; Pruet et al. 2003), or both (e.g., Vlahakis et al. 2003).

A detailed treatment of the process has been presented in § 2 of Fan & Wei (2004b). A novel effect taken into account here is the inverse Compton cooling of the electrons due to the spacetime overlap between the proton shell–neutron shell interaction region and the prompt MeV γ-ray photon flow (see, e.g., Beloborodov 2005; Fan et al. 2005). The inverse Compton (IC) parameter is calculated as $Y = P_{\rm IC}/P_{\rm syn}$, where $P_{\rm IC}$ is the energy-loss rate of one electron by means of IC scattering with the prompt γ-ray emission and $P_{\rm syn} = (4/3)\sigma_{\rm T}(\gamma_e^2 - 1)U_B c$ is the energy-loss rate of one electron by means of synchrotron radiation, with $\sigma_{\rm T}$ the Thomson cross section, γ_e the random Lorentz factor of the emitting electron, and U_B the magnetic energy density generated during the interaction. Since the Klein-Nishina correction is important for the IC process discussed here, we strictly use equations (2.47)–(2.51) and (2.56) from Blumenthal & Gould (1970) to calculate $P_{\rm IC}$. The photon number distribution of the prompt γ-rays is taken to be $n_{\epsilon_\gamma} = n_{\epsilon_\gamma^b}(\epsilon_\gamma/\epsilon_\gamma^b)^{-3/2}$ for $\epsilon_\gamma^b/50 < \epsilon_\gamma < \epsilon_\gamma^b$ and $n_{\epsilon_\gamma} = n_{\epsilon_\gamma^b}(\epsilon_\gamma/\epsilon_\gamma^b)^{-2.25}$ for $\epsilon_\gamma^b < \epsilon_\gamma < 50\epsilon_\gamma^b$, where $\epsilon_\gamma^b \sim 250$ keV is the peak energy of the observed spectrum[5] and $n_{\epsilon_\gamma^b}$ is constrained by the condition $\int n_{\epsilon_\gamma}\epsilon_\gamma\, d\epsilon_\gamma = U_\gamma$, with $U_\gamma \approx L_\gamma/4\pi R^2\gamma^2 c$ the initial γ-ray photon energy density, γ the evolving bulk LF of the proton shell during the sweeping process,[6] and L_γ the prompt γ-ray luminosity.

We calculated the synchrotron light curves for a proton shell interacting with the decay products of a series of slow neutron shells. The result is shown in Figure 1. The following parameters were adopted: $M_p = 3.7 \times 10^{26}$ g is the rest mass of one proton shell; $M_n^0 = 10^{26}$ g is the initial rest mass of one neutron shell; $\Gamma_m = 600$; $\Gamma_{n,s} = 50$ (with these parameters, we obtain $\gamma \simeq 300$ at the end of the interaction; this will be regarded as the initial Lorentz factor in the afterglow phase, and we rewrite it as η in § 3—this matches the value found in our modeling of the early K_s-band afterglow [see § 3]); $\delta t = 10^{-2} \times (1 + z)$ seconds; $D_L = 2.2 \times 10^{28}$ cm is the luminosity distance; $L_\gamma = 10^{52}$ ergs s^{-1}; and $\varepsilon_e = 0.3$ and $\varepsilon_B = 0.1$ are the fraction of shock energy given to the shocked electrons and the magnetic field, respectively. The light curves peak as the observed frequency $\nu_{\rm obs}$ crosses the synchrotron self-absorption frequency ν_a, and another break during the decay phase marks the epoch when $\nu_{\rm obs}$ crosses the typical synchrotron radiation frequency. The ν_a is much smaller than that in the standard internal-shock model, for the following reasons: First, we have $R \gg R_{\rm int}$. Second, the forward-shock upstream proton number density is much smaller than that in standard internal shocks (see eq. [1] of Fan & Wei 2004b for details), which results in a smaller B' and weaker synchrotron emission. Finally, with the effect of IC cooling taken into account, and since synchrotron emission is weaker, the Y-parameter is large, by some tens to hundreds with the typical parameters. The synchrotron radiation luminosity is further lowered by a factor $1/Y$.

The detected flux should be the integrated emission powered by a series of proton shells interacting with the decay trail of slow neutron shells. For $\nu_{\rm obs} = (1.4, 1.8, 2.2, 4.3, 10.0) \times 10^{14}$ Hz, the predicted fluxes are 18.8, 21.2, 23.3, 26.3, and 27.2 mJy, respectively. Such strong emission is detectable with current telescopes and is consistent with the optical observation of GRB 041219a when the extinction correction is taken into account (Vestrand et al. 2005). The averaged spectrum is flat,

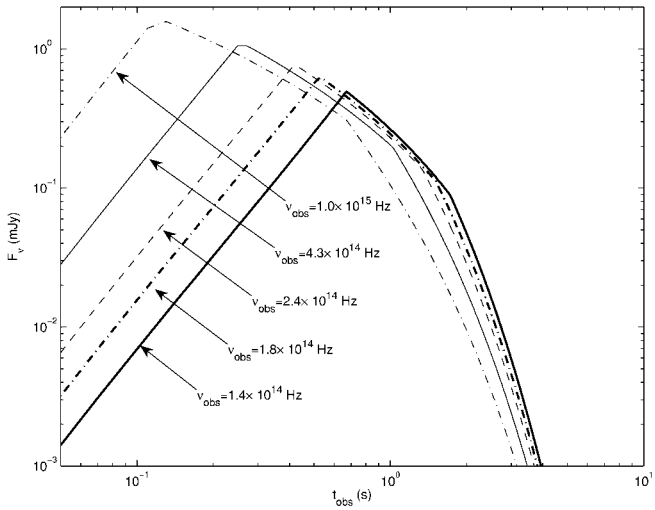

FIG. 1.—Long-wavelength emission (the observer frequency has been marked) powered by a proton shell interacting with the decay products of a series of slow neutron shells as a function of time (similar to Fig. 2 of Fan & Wei 2004b). The following parameters are adopted: $M_p = 3.7 \times 10^{26}$ g, $M_n^0 = 10^{26}$ g, $\Gamma_m = 600$, $\Gamma_{n,s} = 50$, $\delta t = 10^{-2}(1 + z)$ s, $D_L = 2.2 \times 10^{28}$ cm, $\varepsilon_e = 0.3$, $\varepsilon_B = 0.1$, $L_\gamma = 10^{52}$ ergs s^{-1}, and $\epsilon_\gamma^b = 250$ keV. The real light curve should include the contributions from many proton shells.

which is roughly consistent with the earliest IR-band observation of GRB 041219a (Blake et al. 2005). As mentioned in Fan & Wei (2004b), the predicted long-wavelength emission is expected to be correlated with the prompt γ-ray emission but to have a $\sim 10(1 + z)\Gamma_{n,s,1.7}^{-1}$ s lag. This is also consistent with the tracking behavior of the prompt optical flashes (Vestrand et al. 2005). Note that it is not our intention to fit the prompt optical and near-IR emission light curves closely (which requires additional complicated assumptions about the central engine's behavior). The main purpose of the current discussion is to indicate that the neutron-rich internal shock model suffers fewer constraints than the proton-dominated internal shock model and can better account for the observed prompt optical-IR spectrum.

3. THE VERY EARLY NEAR-INFRARED AFTERGLOW

After the internal-shock phase, as the fireball is decelerated by the circumburst medium, a pair of shocks usually develops (Mészáros & Rees 1997; Sari & Piran 1999). The early optical afterglow light curve is usually composed of the contributions from both the forward and the reverse shock. Zhang et al. (2003) pointed out that, depending on parameters, there are two types of early optical-IR light curve for a fireball interacting with a constant-density interstellar medium (ISM), that is, type I (rebrightening), in which distinct reverse-shock and forward-shock peaks are detectable, and type II (flattening), in which the forward-shock (FS) peak is buried beneath the reverse-shock (RS) peak. The previous two strong cases of RS emission (GRB 990123, Akerlof et al. 1999; GRB 021211, Fox et al. 2003 and Li et al. 2003) all belong to type II. Visual inspection of the early IR light curve of GRB 021219a (Blake et al. 2005; see also Fig. 2) indicates that it is a clear type I case. Below we will model the light curve in detail and show that the data are indeed consistent with such an explanation.

Following the standard afterglow model for a fireball interacting with a constant-density medium (e.g., Piran 1999), we write the cooling frequency ν_c^f, the typical synchrotron frequency ν_m^f, and the maximum spectral flux $F_{\nu,\max}^f$ of the

[5] Given the same ϵ_γ^b, the calculated results are not very sensitive to the photon spectral indices assumed.

[6] Note that we have adopted the same symbols as in Fan & Wei (2004b) to maintain consistency between the two papers.

FS emission: $\nu_c^f = 1.4 \times 10^{14} E_{\rm iso,54}^{-1/2} \varepsilon_{B,-2}^{-3/2} n_0^{-1} t_d^{-1/2} [2/(1+z)]$ Hz, $\nu_m^f = 1.8 \times 10^{13} E_{\rm iso,54}^{1/2} \varepsilon_{B,-2}^{1/2} \varepsilon_{e,-0.5}^{2} t_d^{-3/2} C_p^2 [2/(1+z)]$ Hz, and $F_{\nu,\max}^f = 83 E_{\rm iso,54} \varepsilon_{B,-2}^{1/2} n x_0^{1/2} D_{L,28.34}^{-2} [(1+z)/2]$ mJy, where $C_p = 7(p-2)/[2(p-1)]$, $E_{\rm iso}$ is the isotropic energy of the outflow, ε_e and ε_B are the fractions of the shock energy given to electrons and to magnetic fields in the forward shock, respectively, n is the number density of the external medium, and $p \sim 2.4$ is the power-law distribution index of the shocked electrons. Hereafter $t = t_{\rm obs}/(1+z)$ denotes the observer's time corrected for the effect of cosmological time dilation and t_d is in units of days. The superscripts "f" and "r" denote the FS and RS emission, respectively. We assume that ε_e and the electron spectral index p are essentially the same for both the FS and RS,[7] but we will allow different ε_B-values for both regions. One reason for this assumption is that the magnetic field generated in the internal-shock phase may have not been dissipated effectively in a short time and would play a dominant role in the reverse-shock region (Fan et al. 2004 and references therein). In this Letter, we will write $\varepsilon_B^f = \varepsilon_B$ and $\varepsilon_B^r = \mathcal{R}_B^2 \varepsilon_B$, where $\mathcal{R}_B$ is the ratio of the magnetic field in the RS emission region to that in the FS emission region (Zhang et al. 2003). Previous analyses have indicated that at least for some bursts (e.g., GRB 990123 and GRB 021211), the RS emission region is more magnetized than the FS region (e.g., Fan et al. 2002; Zhang et al. 2003; Kumar & Panaitescu 2003).

As shown in Figure 2 (data taken from Blake et al. 2005; only the richest K_s-band data are plotted), the time when the RS crosses the ejecta [$(1+z)t_\times$] is about 30 minutes after the trigger, which is much longer than $T_{90} \sim 520$ s. So, the RS is nonrelativistic (see, e.g., Sari & Piran 1995; Kobayashi 2000; Kobayashi & Zhang 2003). Further evidence for a nonrelativistic RS is the rapid increase of the early afterglow light curve (e.g., Kobayashi 2000; Kobayashi & Zhang 2003). The LF of the decelerated outflow relative to the initial LF at $t_\times$, $\gamma_{34,\times} \approx (\eta/\Gamma_\times + \Gamma_\times/\eta)/2$, can be estimated by solving $c\,dt/d\Delta \approx (1-\beta_{\Gamma_3})\{1-\eta/[\Gamma_3(4\gamma_{34}+3)]\}/(\beta_\eta - \beta_{\Gamma_3})$ numerically (e.g., Sari & Piran 1995; Fan et al. 2004). Here Γ_3 is the bulk LF of the shocked ejecta, η is the initial bulk LF of the outflow, $\Gamma_\times$ is the LF of the decelerated ejecta at $t_\times$, and β_A is the corresponding velocity (in units of c) of the LF Γ_A. For GRB 041219a, one has $t_\times \sim 4T_{90}/(1+z)$, so that $\gamma_{34,\times} - 1$ is much smaller than 1, that is, the RS is nonrelativistic. In such a case, $t_\times$ can be approximated as

$$t_\times \approx 64 E_{\rm iso,54}^{1/3} n_0^{-1/3} \eta_{2.5}^{-8/3} \ {\rm s}. \quad (1)$$

The typical frequency of the RS emission is

$$\nu_m^r(t_\times) = \mathcal{R}_B(\gamma_{34,\times} - 1)^2 \nu_m^f(t_\times)/(\Gamma_\times - 1)^2, \quad (2)$$

Following Zhang et al. (2003), we have

$$\nu_c^r \approx \mathcal{R}_B^{-3} \nu_c^f, \quad F_{\nu,\max}^r(t_\times) \approx \eta \mathcal{R}_B F_{\nu,\max}^f(t_\times). \quad (3)$$

Generally, the K_s-band flux satisfies $F_{\nu_{K_s}} \approx F_{\nu,\max}^r(t_\times)[\nu_{K_s}/\nu_m^r(t_\times)]^{-(p-1)/2}$.

Assuming $z = 1$, $p = 2.4$, and $E_{\rm iso,54} = 1$ (consistent with the γ-ray fluence and our assumed redshift), ε_e, n, and η can be constrained by the following two conditions: (1) at $t_d \sim 0.14$, $\nu_m^f \sim \nu_{K_s}$, and $F_{\nu,\max}^f \sim 0.6$ mJy; (2) $t_\times$ is about $30/(1+z)$ minutes. We then find

$$\varepsilon_e \sim 0.2 \varepsilon_{B,-2}^{-1/4}, \quad n \sim 5 \times 10^{-5} \varepsilon_{B,-2}^{-1}, \quad \eta \sim 380 \varepsilon_{B,-2}^{1/8}. \quad (4)$$

It is interesting to see that since $\varepsilon_e < 1$, we have $\varepsilon_B > 1.6 \times 10^{-5}$, $n < 3 \times 10^{-2}$ cm^{-3}, and $\eta > 170$. The parameter $\mathcal{R}_B$ can be constrained by noting that $F_{\nu_{K_s}}((1+z)t_\times) \sim 2.4$ mJy and taking $\eta \sim 380$, which yields

$$\mathcal{R}_B \sim 3[(\gamma_{34,\times} - 1)/0.2]^{-14/17}, \quad (5)$$

hinting that the reverse-shock region is mildly magnetized.

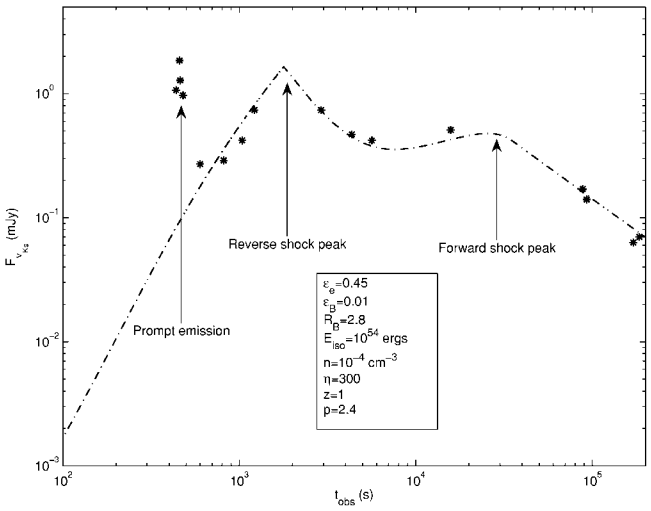

FIG. 2.—Modeling the K_s-band afterglow data of GRB 041219a. The data are taken from Blake et al. (2005). The earliest data are prompt emission, which is not included in our fit. The dash-dotted line is the theoretical light curve. Both the reverse-shock and the forward-shock emission components are included. The best-fit parameters are listed.

Following Fan et al. (2005), the forward-reverse shock emission has been calculated numerically. Since the RS is nonrelativistic, the spreading of the ejecta (see, e.g., Piran 1999) has been taken into account. The fits to the K_s-band data are presented in Figure 2. We find that the data can be well modeled with the following parameters: $z = 1$, $E_{\rm iso,54} = 1$, $\varepsilon_e = 0.45$, $\varepsilon_B = 0.01$, $\mathcal{R}_B = 2.8$, $\eta = 300$, and $n = 10^{-4}$ cm^{-3}. These are consistent with the analytical estimates above.

There are three radio data points available (Soderberg & Frail 2004; van der Horst et al. 2004a, 2004b). The 8.5 GHz flux at 1.1 days is 0.45 mJy, and the 4.9 GHz flux at 1.6 and 2.6 days is 0.2 and 0.34 mJy, respectively. By taking our best-fitting parameters, the corresponding FS fluxes are ~0.04, ~0.04, and ~0.05 mJy, respectively, too low to interpret the data. When we consider the RS contribution to the radio band (see, e.g., Sari & Piran 1999; Kobayashi & Zhang 2003; Gou et al. 2004), the overall corresponding fluxes become ~0.60, ~0.37, and ~0.18 mJy, respectively, roughly matching the data. Therefore, the radio data also support the reverse-forward shock interpretation.

4. SUMMARY AND DISCUSSION

The prompt optical-IR observations of GRB 041219a (Vestrand et al. 2005; Blake et al. 2005) offer a great opportunity to diagnose the unknown composition of GRB ejecta. We have shown that the prompt optical emission tracking the γ-ray emis-

[7] If they are different, additional corrections are needed; see Zhang et al. (2003) and Zhang & Kobayashi (2005) for details.

sion profile may be consistent with a picture in which the ejecta is neutron-rich and the optical emission is powered by the proton shells interacting with the neutron decay products at a distance farther away from the central engine than the typical internal-shock radius.

By modeling the K_s-band early afterglow light curve, we identify a reverse-shock emission component, which is clearly separated from the forward-shock emission component. Such a rebrightening (type I) light curve was expected by Zhang et al. (2003) to be more common if the RS is not strongly magnetized. Indeed, detailed modeling indicates that $\mathcal{R}_B$ in GRB 041219a is, at most, mild, in contrast with GRB 990123 and GRB 021211 (e.g., Fan et al. 2002; Zhang et al. 2003; Kumar & Panaitescu 2003). This is also consistent with the neutron-rich picture conjectured in interpreting the prompt optical emission. The mild magnetization of the ejecta may be due to magnetic field generation during the internal-shock phase. The radio data also support our reverse-forward shock interpretation.

It is interesting to note that for the three bursts with reverse-shock identifications (GRB 990123, 021211, and 041219a), the inferred number densities of the ISM are typically lower than the standard value of $n \sim 1$ cm^{-3} (see also Kumar 2004): for GRB 990123, $n \sim 10^{-3}$ cm^{-3} (e.g., Wang et al. 2000; Panaitescu & Kumar 2002; Nakar & Piran 2004); for GRB 021211, $n \sim 10^{-3}$ to 10^{-2} cm^{-3} (e.g., Wei 2003; Kumar & Panaitescu 2003); and for the current GRB 041219a, $n \sim 10^{-4}$ cm^{-3}. The reason is unclear, but certain selection effects may play a role.

We thank L.-J. Gou and X.-F. Wu for helpful discussions, and the referee for valuable comments. This work was supported by NASA grant NNG04GD51G and the NASA *Swift* Guest Investigator (Cycle 1) program (B. Z.), the National Natural Science Foundation of China (grants 10073022, 10225314 and 10233010), and the National 973 Project on fundamental research in China (NKBRSF G19990754) (D. M. W.).

REFERENCES

Akerlof, C., et al. 1999, Nature, 398, 400
Barthelmy, S., et al. 2004, GCN Circ. 2874, http://gcn.gsfc.nasa.gov/gcn/gcn3/2874.gcn3
Beloborodov, A. M. 2003, ApJ, 588, 931
———. 2005, ApJ, 618, L13
Blake, C. H., et al. 2005, Nature, 435, 181
Blumenthal, G. R., & Gould, R. J. 1970, Rev. Mod. Phys., 42, 237
Derishev, D. E., Kocharovsky, V. V., & Kocharovsky, V. V. 1999, ApJ, 521, 640
Fan, Y. Z., Dai, Z. G., Huang, Y. F., & Lu, T. 2002, Chinese J. Astron. Astrophys., 2, 449
Fan, Y. Z., & Wei, D. M. 2004a, MNRAS, 351, 292
———. 2004b, ApJ, 615, L69
Fan, Y. Z., Wei, D. M., & Wang, C. F. 2004, A&A, 424, 477
Fan, Y. Z., Zhang, B., & Wei, D. M. 2005, ApJ, 628, 298
Fox, D. W., et al. 2003, ApJ, 586, L5
Gotz, D., Mereghetti, S., Shaw, S., Beck, M., & Borkowski, J. 2004, GCN Circ. 2866, http://gcn.gsfc.nasa.gov/gcn/gcn3/2874.gcn3
Gou, L.-J., Mészáros, P., Abel, T., & Zhang, B. 2004, ApJ, 604, 508
Katz, J. I. 1994, ApJ, 432, L107
Kobayashi, S. 2000, ApJ, 545, 807
Kobayashi, S., & Zhang, B. 2003, ApJ, 582, L75
Kumar, P. 2004, in Proc. 22nd Texas Symp. on Relativistic Astrophysics, ed. P. Chen et al. (Stanford: SLAC), No. 0032
Kumar, P., & Panaitescu, A. 2003, MNRAS, 346, 905
Li, W., Filippenko, A. V., Chornock, R., & Jha, S. 2003, ApJ, 586, L9
Li, Z., & Song, L.-M. 2004, ApJ, 608, L17
Lyutikov, M., & Blandford, R. D. 2003, preprint (astro-ph/0312347)
Mészáros, P., & Rees, M. J. 1997, ApJ, 476, 232
———. 1999, MNRAS, 306, L39
Nakar, E., & Piran, T. 2004, MNRAS, 353, 647
Paciesas, W., et al. 1999, ApJS, 122, 465
Panaitescu, A., & Kumar, P. 2002, ApJ, 571, 779
Piran, T. 1999, Phys. Rep., 314, 575
Pruet, J., Woosley, S. E., & Hoffman, R. D. 2003, ApJ, 586, 1254
Sari, R., & Piran, T. 1995, ApJ, 455, L143
———. 1999, ApJ, 517, L109
Schaefer, B. E., et al. 1994, ApJ, 422, L71
Soderberg, A. M., & Frail, D. A. 2004, GCN Circ. 2881, http://gcn.gsfc.nasa.gov/gcn/gcn3/2881.gcn3
van der Horst, A. J., Rol, E., & Strom, R. 2004a, GCN Circ. 2894, http://gcn.gsfc.nasa.gov/gcn/gcn3/2894.gcn3
———. 2004b, GCN Circ. 2895, http://gcn.gsfc.nasa.gov/gcn/gcn3/2895.gcn3
Vestrand, W. T., et al. 2005, Nature, 435, 178
Vlahakis, N., Peng, F., & Königl, A. 2003, ApJ, 594, L23
Wang, X.-Y., Dai, Z.-G., & Lu, T. 2000, MNRAS, 319, 1159
Wei, D.-M. 2003, A&A, 402, L9
Wei, D.-M., & Cheng, K. S. 1997, MNRAS, 290, 107
Zhang, B., & Kobayashi, S. 2005, ApJ, 628, 315
Zhang, B., Kobayashi, S., & Mészáros, P. 2003, ApJ, 595, 950